



27 studied, also featured good thermal and daylighting performances. The PV-DSF can  
28 effectively block solar radiation while still providing considerable daylighting illuminance.  
29 Due simply to excellent overall energy performance, a PV-DSF at Berkeley can reduce  
30 net electricity use by about 50% compared with other commonly used glazing systems.  
31 Efficiency improvements of semi-transparent PV modules would further increase the  
32 energy saving potential of a PV-DSF and thus making this technology more promising

33 **Keywords:** building-integrated photovoltaic (BIPV), energy saving potential, building  
34 energy use, double-skin facade, semi-transparent thin-film photovoltaic (STPV)

### 35 **1. Introduction**

36 In the U.S. during 2010, approximately 41% of total energy consumption was spent in  
37 residential and commercial buildings. Heating, ventilating and air conditioning (HVAC)  
38 accounted for more than 50% of the total building energy use [1]. Thus, economically  
39 and in the interests of sustainability, energy saving in this area is of value. An effective  
40 way to reduce building energy consumption, but still ensuring the comfort and  
41 convenience of the building users, is by the reduction of heat transfer throughout the  
42 building envelope, and thereby reducing cooling/heating loads. Given that windows and  
43 glazing facades, for instance, usually have poor thermal insulation properties, the  
44 development of energy efficient curtain walls/facades could considerably reduce heat  
45 transfer from outside to the inside of buildings. In recent years, semi-transparent thin-film  
46 PV (STPV) windows/facades have been a focus of research interest due to their energy  
47 efficient performance levels [2-13]. STPV windows/facades not only generates electricity  
48 in situ through photovoltaic effect but also significantly reduces the air-conditioning  
49 cooling load by blocking solar heat gain [14-19]. Additionally, STPV windows with

50 appropriate transmittance also enable full use of daylighting [15, 20-23]. Much research  
51 related to the overall energy performance of STPV windows/facades has been conducted  
52 with the objective of determining their energy saving potential. Both experimental and  
53 simulation methods have been used and reported.

54 A comprehensive energy analysis has been conducted for semi-transparent building-  
55 integrated photovoltaic (BIPV) windows in Singapore [24]. To evaluate the overall  
56 energy performance in this instance, an index of net electrical benefits (NEB) including  
57 the generation of electricity, the reductions of cooling energy and artificial lighting  
58 energy was introduced. As a result, a better NEB was determined involving high PV  
59 efficiency and good thermal properties. In Singapore, when compared with other  
60 commonly used glazing systems, semi-transparent BIPV windows were found to be the  
61 best in terms of overall energy saving performance providing the window-wall-ratio was  
62 optimized in keeping with the various possible orientations. Li et al. [25] investigated the  
63 energy performance of a semi-transparent a-Si PV facade for a generic reference office  
64 building in Hong Kong. The simulation results showed that semi-transparent PV modules  
65 were able to reduce the annual building electricity use and peak cooling load by  
66 1203MWh and 450kW, respectively, if combined with a dimmable lighting control  
67 system. Previous study reported that electricity generation of STPV window was  
68 relatively small, however, it worked as an efficient sun shading in summer and thus  
69 giving a potential for the reduction of investments for cooling equipment and savings on  
70 cooling energy use [26].

71 In Spain, the STPV facade energy saving potential based on different window-to-wall  
72 ratios and different transmittances was evaluated by Olivieri et al [27]. The saving ranged

73 from 18% to 59% compared to that of a normal glazing. Didone and Wagner [28]  
74 evaluated the energy saving potential of STPV windows in Brazil via simulation. The  
75 simulation results indicated that the STPV window has a considerable potential for  
76 reducing lighting and air-conditioning energy if used with appropriate control strategies.  
77 The impacts of optical characteristics on the overall energy performance of STPV  
78 windows have also been investigated by Chae et al [29]. It was found that the optical  
79 response at each wavelength could significantly affect the thermal, power and daylighting  
80 performance or availability. To maximize the energy saving potential of STPV windows,  
81 it seems necessary for the optical characteristics to be customized when fabricating PV  
82 laminates. Kapsis and Athienitis [30] examined the impact of various building design  
83 parameters on the selection of ideal optical properties for STPV windows. It was reported  
84 that STPV windows with 10% visible transmittance had the best energy saving potential.

85 Previous studies have also reported the thermal insulation performance of single-skin  
86 STPV windows to be unsatisfactory because of high heat gain coefficients in summer and  
87 serious heat loss during winter nights [31]. A significant reduction of U-value could make  
88 PV window become one of the most energy efficient window alternatives [32]. To  
89 achieve this goal, ventilated double-skin STPV windows of various types were proposed  
90 and their thermal performances studied. Chow et al. [33] investigated the thermal  
91 performance of a naturally-ventilated STPV window together with the impact on air-  
92 conditioning cooling load reduction. The heat transfer and airflow in the ventilation  
93 cavity were simulated using the ESP-r simulation platform, separating the cavity into  
94 several thermal zones. The simulation results showed that the naturally-ventilated PV  
95 glazing, when compared to the common absorptive glazing window in Hong Kong, could

96 reduce the annual air-conditioning energy use by 28%. Brandl et al. investigated the  
97 ventilation effect and thermal behavior of a BIPV façade with 3D CFD models [34]. Due  
98 to periphery openings, heat in the cavity was partly transferred to the exterior under the  
99 effects of natural ventilation. The thermal performances of single-skin and double-  
100 glazing STPV windows were compared using a hot-box designed for that purpose [35].  
101 The experimental results indicated that, in East China, a double-glazing STPV window  
102 could reduce the indoor heat gain to 46.5% of that of a single-skin PV window. More  
103 importantly, the thermal comfort in the room was obviously better, as the inner surface  
104 temperature of the double-glazing STPV window was much lower than that of the single-  
105 glazing one. Elarga et al. [36] conducted a dynamic numerical analysis of the cooling  
106 energy performance of a ventilated BIPV façade with semitransparent PV cells inside the  
107 façade cavity. It was found that the integration of solar cells inside the façade cavity  
108 enabled the HVAC system to cool down the PV modules, which not only increased the  
109 energy conversion efficiency but also extend the life time of the system.

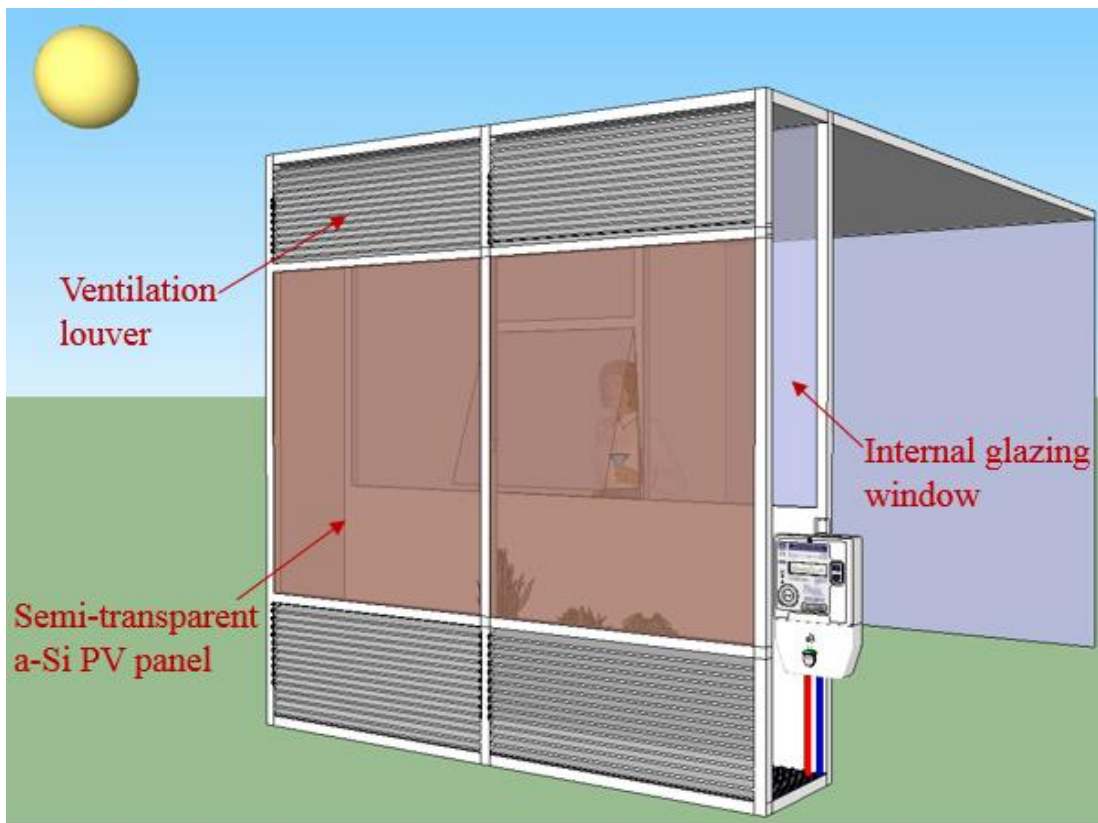
110 A novel ventilated photovoltaic double-skin facade (PV-DSF) was developed and has  
111 been presented in the authors' previous studies. Its thermal and power performances  
112 under different ventilation modes were demonstrated during long term outdoor testing  
113 [37-38]. The experimental results showed that the average solar heat gain coefficient  
114 (SHGC) of the ventilated PV-DSF was less than 0.15, a measurement which is far less  
115 than that of a single-skin STPV window. In addition, it was found that a ventilated PV-  
116 DSF could improve the daily energy output by a further 3%, a result based on its lower  
117 operating temperature.

118 From literature reviews, it is evident that although the energy saving potential of single-  
119 skin STPV windows has received much attention worldwide, the saving potential of  
120 double-glazing STPV windows has, in comparison, rarely been studied and reported. In  
121 the study reported in this paper, a comprehensive simulation model based on EnergyPlus  
122 is introduced to simulate the year round overall energy performance of a ventilated PV-  
123 DSF, situated in the cool-summer Mediterranean climate of Berkeley, California.  
124 Weather data, of a typical meteorological year (TMY) was used in the simulation. Based  
125 on the simulation model, sensitivity analyses of air gap depths and various ventilation  
126 modes were conducted to optimize the design of the PV-DSF structure and the  
127 operational strategy. For the optimized PV-DSF, the annual power generation, thermal  
128 and daylighting performances were comprehensively investigated. The monthly overall  
129 energy performance and net electricity use were also calculated. A study, comparing the  
130 PV-DSF and commonly used window glazing, was then conducted, with the aim of  
131 revealing the energy saving potential of the PV-DSF in cool-summer Mediterranean  
132 climate zones.

## 133 **2. PV-DSF and Simulation Model**

134 As shown in Figure 1, the PV-DSF consists of an outside layer of semi-transparent a-Si  
135 PV panels, an inner layer of an openable window as well as an intermediate 400 mm air  
136 ventilation cavity. This PV-DSF possesses the following merits. Firstly, the inside  
137 openable window makes air exchange and solar passive heating possible, when needed.  
138 Secondly, as the PV panels are semi-transparent, with transmittance of about 7%, thus  
139 enabling some natural daylight to penetrate the PV panels and illuminate the room. The  
140 upper ventilation louvres can further significantly improve indoor daylighting because

141 daylight can pass through the grille gaps and enter the room. Of final importance is the  
142 ventilation design. As shown in Figure 1, cold air can enter the airflow cavity through the  
143 bottom inlet louvre, exchange heat with the PV panels as well as the inside windows and  
144 finally exhaust a considerable amount of waste heat via the upper outlet louvre. Previous  
145 experimental studies demonstrated that such ventilation not only reduces the cooling load  
146 by 15%, but also enhances the PV module's energy output by about 3% [37-38]. The key  
147 parameters of the PV-DSF are listed in Table 1. More information about this particular  
148 PV-DSF is available in [37-38]. The physical characteristics of the semi-transparent PV  
149 panels used in the PV-DSF are given in Table 2.



150

151

152

153

**Figure 1** Schematic diagram of the PV-DSF

**Table 1** Key dimensions of the ventilated PV-DSF system

<b>Parameters</b>	<b>Values</b>
Width of PV panel	1.1 m
Height of PV panel	1.3 m
Thickness of PV module	0.006 m
Width of louver	1.1 m
Height of louver	0.45 m
Depth of air flow duct	0.4 m
Dimension of office room (W*L*D)	2.3*2.5*2.2 m

154  
155  
156

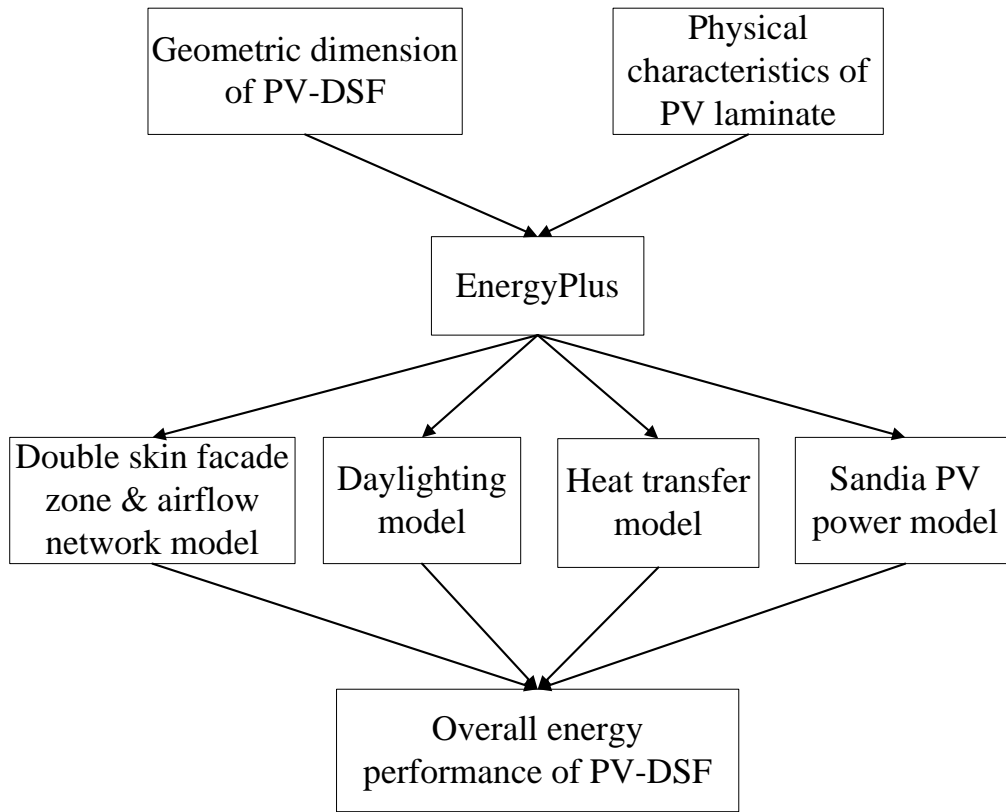
**Table 2** Physical characteristics of the semi-transparent a-Si PV panel

<b>Parameters</b>	<b>Values</b>
Maximum power under STC ( $W_p$ )	85
Open circuit voltage, $V_{oc}$ (V)	134.4
Short circuit current, $I_{sc}$ (A)	1.05
Voltage at the maximum power point, $V_{mp}$ (V)	100
Current at the maximum power point, $I_{mp}$ (A)	0.85
Efficiency, $\eta$ (%)	6.2
Power temperature coefficient ( $T_k$ )	-0.21%/K
Dimensions (L*W*D), (mm)	1300×1100×7
Transmittance in Visible lighting range	7%
Thermal conductivity, ( $Wm^{-1}K^{-1}$ )	0.486
Infrared emittance	0.85

157



158 To investigate the overall energy performance as well as the energy saving potential of  
159 the PV-DSF, a comprehensive simulation model was developed based on EnergyPlus.  
160 Figure 2 illustrates the simulation work flowchart. The work was started by measuring  
161 the physical characteristics of the semi-transparent a-Si PV module, including its optical  
162 characteristics, infrared thermal emissivity and thermal conductivity. The measured  
163 physical characteristics were input into the Window program to create a physical  
164 characteristics file which can be read by EnergyPlus. The Window program is an  
165 example of professional software for calculating the thermal and optical properties of  
166 glazing and window systems [39]. The physical characteristics file created by Window  
167 was then imported into EnergyPlus together with the PV-DSF geometric dimensions. In  
168 EnergyPlus, different models and sub-models, such as the airflow network model,  
169 daylighting model, heat transfer model and the Sandia PV power model, were employed  
170 to simultaneously simulate the power, thermal and daylighting performances of the PV-  
171 DSF.



172

173 **Figure 2** Flowchart of simulating the overall energy performance of PV-DSF

174 The Airflow Network model was adopted to simulate the heat transfer and air flow in the  
 175 ventilation cavity to investigate the impacts of ventilation on both the power performance  
 176 improvement and the cooling load reduction. The Daylighting model in EnergyPlus was  
 177 chosen to simulate the daylighting performance of PV-DSF under different weather and  
 178 sky conditions, such as cloudy, overcast, bright sunlight, as well as to investigate the  
 179 impact on lighting energy use. For power output simulation, the Sandia Array  
 180 Performance Model (SAPM) was employed. Although the Sandia model is empirically  
 181 based, it can achieve versatility and accuracy for almost all PV technologies, especially  
 182 for thin-film solar cells, because all the coefficients used in this model are derived from  
 183 special tests using the same kind of solar cells [40-41]. In addition, this model also takes  
 184 into account many factors which considerably affect the power output of PV modules,

185 such as the operating temperature, sunlight incidence angle, solar spectrum and optical  
186 effects [42-43].

### 187 **3. Model Validation**

188 The PV-DSF model developed was then validated against experimental data to verify its  
189 accuracy. The outdoor experimental campaign was carried out in the winter of 2012-2013  
190 in Hong Kong. The measured and simulated monthly AC power generations during the  
191 experimental campaign were compared in Table 3. To validate the SAPM model's  
192 accuracy on predicting annual power generation, the model estimates and measured data  
193 were compared using mean-bias-error (MBE), mean-absolute-error (MAE) and root-  
194 mean-square-error (RMSE) statistics, and the results are 0.14%, 2.13% and 2.47%,  
195 respectively.

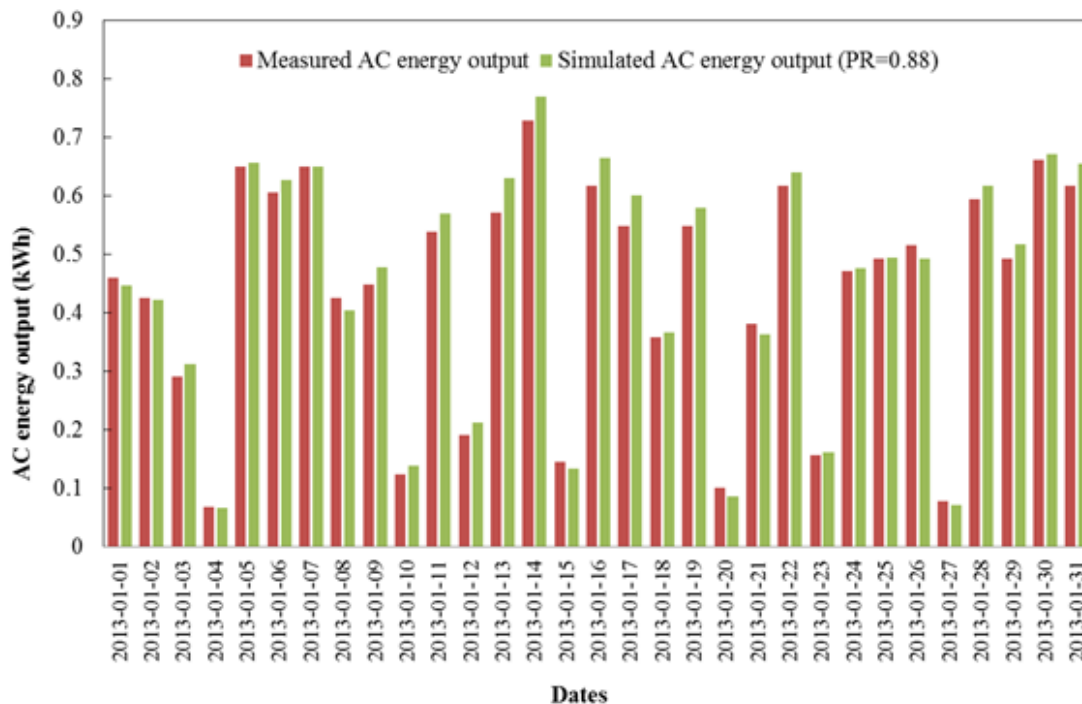
196 **Table 3** Comparison of measured and simulated monthly AC power generation

<b>Months</b>	<b>Measured AC power (kWh)</b>	<b>Simulated AC power (kWh)</b>
<b>October</b>	11.46	11.19
<b>November</b>	7.38	7.4
<b>December</b>	9.12	9.27
<b>January</b>	13.56	13.96
<b>February</b>	8.66	8.43

197

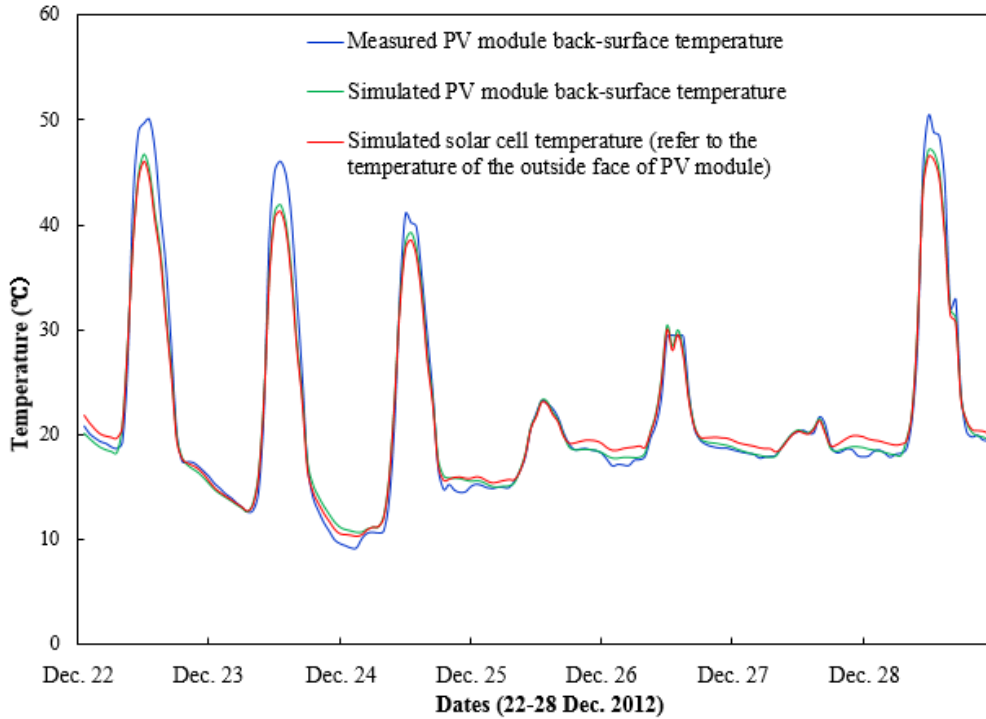
198 Experimental results in January 2013, a typical winter month in Hong Kong, were chosen  
199 to validate against the simulated daily AC energy output. As shown in Figures 3, the  
200 SAPM accurately simulated the daily energy output of the PV-DSF with the 39 special  
201 pre-determined coefficients. The measured monthly AC energy output was 13.56 kWh in  
202 January 2013, while the simulated value was 13.96 kWh, an error of 3%. Such a high

203 level of accuracy for the monthly energy output prediction indicates that the SAPM fully  
 204 qualifies for use in simulating the annual energy output performance of the a-Si PV-DSF.



205  
 206 **Figure 3** Comparison of the simulated daily energy output and the measured one in  
 207 January 2013

208 A comparison of the simulated solar cell temperature and the measured PV module back-  
 209 surface temperature is presented in Figure 4. The measured PV module back-surface  
 210 temperature is a little higher than the simulated solar cell temperature, and the back-  
 211 surface temperature at noon on sunny days, the maximum temperature difference was  
 212 about 3 °C. On overcast days, the simulated temperatures coincided with the measured  
 213 temperatures very well. The MAPEs between the simulated PV module back-surface  
 214 temperatures and the measured results on sunny days (from Dec. 22-24 and Dec.28) and  
 215 overcast days (Dec.25-27) were 6% and 1.7%, respectively.



216

217 **Figure 4** Comparison of the simulated solar cell temperatures and the measured PV

218

module temperature

219 **4. Sensitivity Analysis for PV-DSF in Berkeley**

220 **4.1 Sensitivity Analysis of Air Gap Depth**

221 As given above, the PV-DSF studied was a ventilated-type facade, enabling cold air to

222 enter the cavity via the bottom inlet louvre and exhaust from the upper outlet louvre with

223 removing a considerable amount of waste heat in the process. The air ventilation design

224 not only blocks off heat gain from the exterior to reduce the cooling load, but also

225 improves the PV system energy conversion efficiency by cooling the PV module itself.

226 Thus, an optimal design for the air ventilation cavity is beneficial in both reducing

227 building energy use and increasing the energy output of the PV-DSF. In this study, a

228 sensitivity analysis was conducted to investigate the effect of the air gap depth on the

229 overall energy performance of the PV-DSF in Berkeley, California. Figure 5 presents the

230 variation trends of the annual fan, cooling, lighting and net electricity uses as the air gap  
231 depth increases. The fan and cooling electricity uses increased as the air gap depth  
232 increased to less than 200mm, but decreased when the gap was larger than 200mm. Thus,  
233 200mm proved to be a critical air gap depth at which the least amount of electricity could  
234 be saved. This may be because the PV-DSF stack effect was strengthened by the air gap  
235 depth decreasing to less than 200mm. This latter situation reinforces the heat convection  
236 effect. Under this condition, continually increasing waste heat is removed by the exhaust  
237 air via the outlet louvre. When the air gap depth is greater than 200mm, the air thermal  
238 resistance then gradually increases in relation to the air gap depth, such that the outside  
239 heat gain declines. The lighting electricity use gradually increases with the increasing air  
240 gap depth. The distance between outside and inside daylighting reference points  
241 increased as the air gap depth increased, resulting in a reduction of daylighting  
242 illuminance at the reference points. Thus, more electricity for lighting is needed to  
243 compensate for reductions of daylighting illuminance. The inflection point at 225mm  
244 might be attributed to the slat angle of outlet louvre, which may block natural lighting  
245 penetration to different degrees as the air gap depth changing.

246 Compared with lighting and cooling electricity uses, the impact of the air gap depth on  
247 the PV power generation was very small because the power temperature coefficient of a-  
248 Si PV modules is small (about 0.25%). If crystalline silicon PV modules are to be used,  
249 the impact would be larger because their power temperature coefficients are about twice  
250 that of a-Si PV modules.

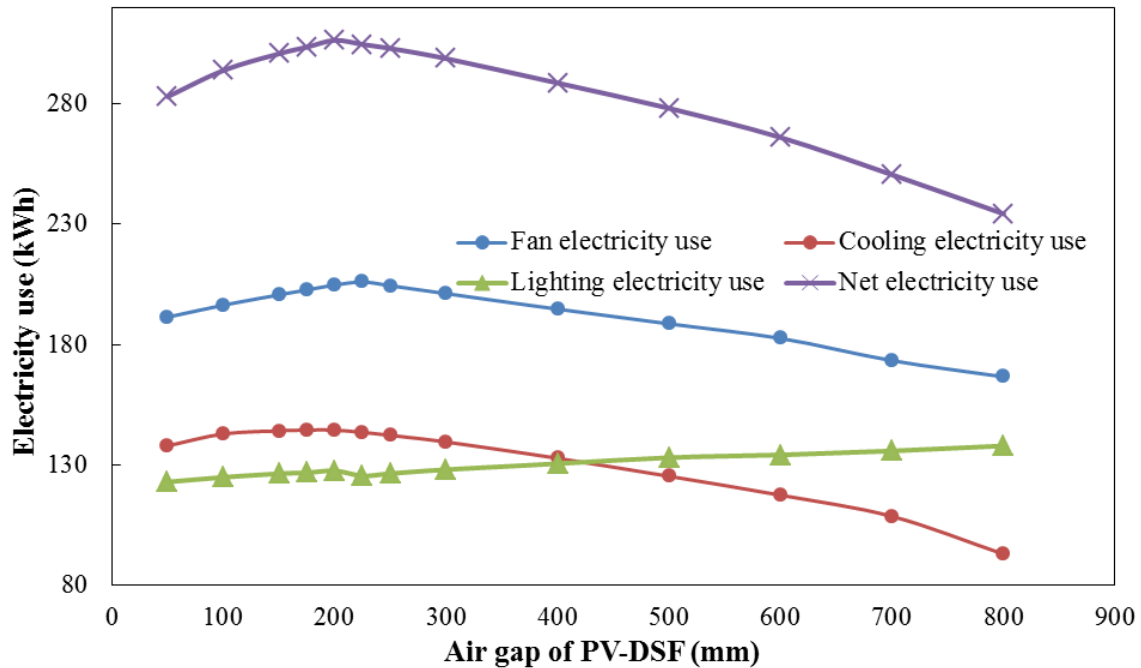


**Figure 5** The impact of air gap depth on the annual electricity uses

251

252

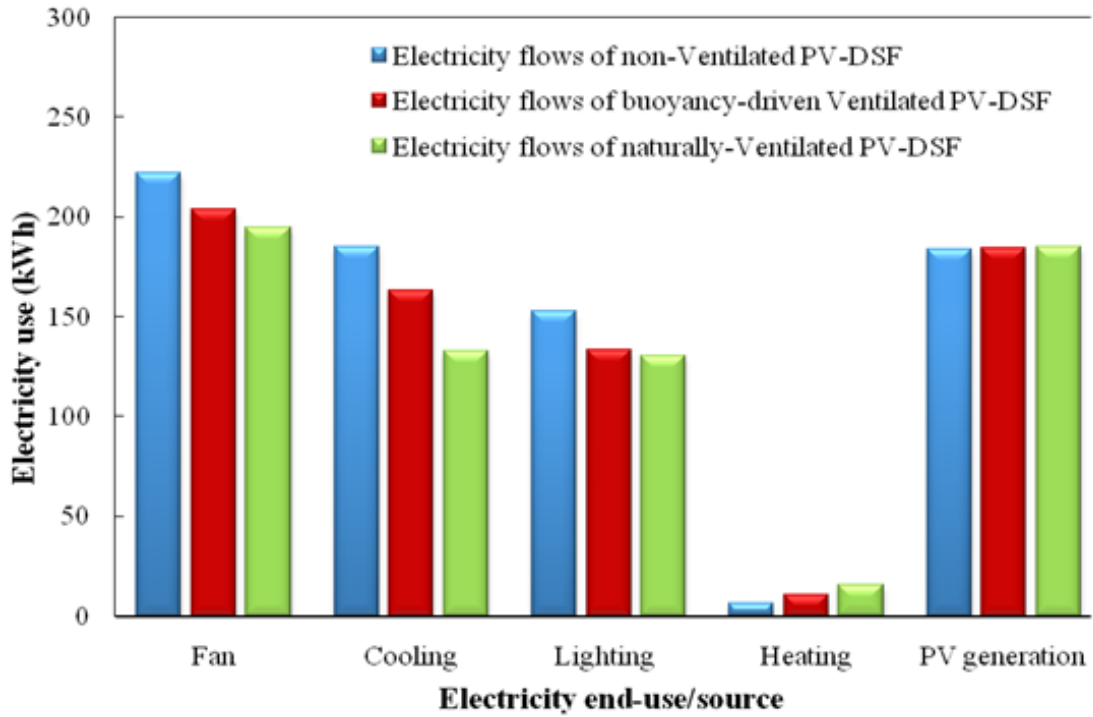
253

254 The impact of air gap depth on the net electricity use of an office room fitted with a PV-  
 255 DSF is also illustrated in Figure 5. It was found that the worst air gap depth for a PV-DSF  
 256 installation in Berkeley is 200 mm, at this distance the room consumes the largest amount  
 257 of annual net electricity. Thus, PV-DSF installations at Berkeley should avoid this air gap  
 258 depth. When the air gap depth was larger than 200mm, the net electricity use decreased  
 259 as the gap increased. Although the net electricity use decrease continues to parallel the air  
 260 gap increase, a tradeoff can be achieved with regard to space provision in the building  
 261 and electricity saving. Thus, after comprehensively considering all aspects, including  
 262 energy use, costs, facade cleaning and maintenance, 400 to 600mm is recommended as an  
 263 ‘optimal’ air gap range for such as Berkeley conditions. The annual net electricity use  
 264 would be reduced by 15% if the air gap depth is chosen to be 600mm rather than 200mm.

### 265 **3.2 Sensitivity Analysis of Ventilation Modes**

266 In order to investigate the impact of air ventilation on the electricity end-uses, the  
267 electricity generated by the PV-DSFs and the electricity used when operating in the three  
268 ventilation modes: non-ventilated, buoyancy-driven ventilated and naturally-ventilated,  
269 were calculated and are shown in Figure 6. It was found that the naturally-ventilated PV-  
270 DSF had greater ability than the non-ventilated PV-DSF to reduce the fan, cooling and  
271 lighting electricity demands. Its usage, however, needs to be somewhat greater in the  
272 case of heating. It is worth noting that the ventilation mode effect on the PV energy  
273 output was not obvious because the power temperature coefficient of a-Si PV modules is  
274 small. Figure 7 illustrates the energy use breakdowns of PV-DSFs under different  
275 ventilation modes. There is no doubt that among the three modes, the naturally-ventilated  
276 PV-DSF consumes the lowest amount of electricity, followed by the buoyancy-driven  
277 ventilated PV-DSF. The non-ventilated PV-DSF was the least efficient. Compared with  
278 the non-ventilated PV-DSF, natural ventilation saves about 35% of electricity per year in  
279 Berkeley. This powerfully makes the point that ventilation design is a necessary and  
280 effective component for PV-DSF in terms of energy saving.



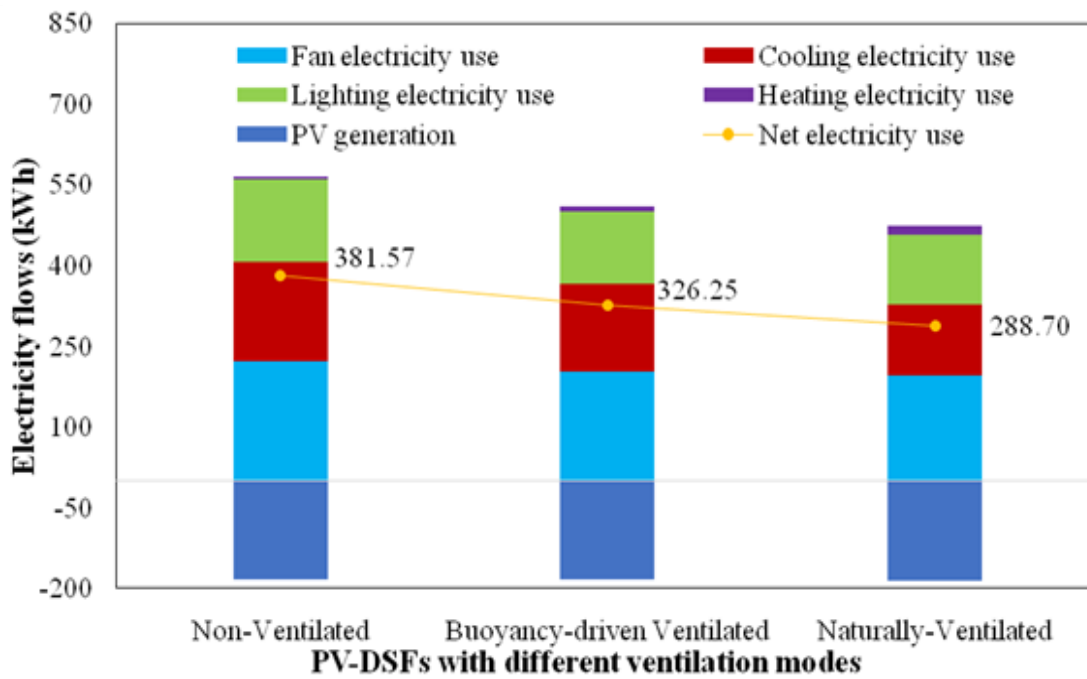


281

282 **Figure 6** Electricity generated and used by PV-DSFs under different ventilation modes in

283

Berkeley



284

285 **Figure 7** Annual net electricity use of PV-DSFs under different ventilation modes in  
286 Berkeley

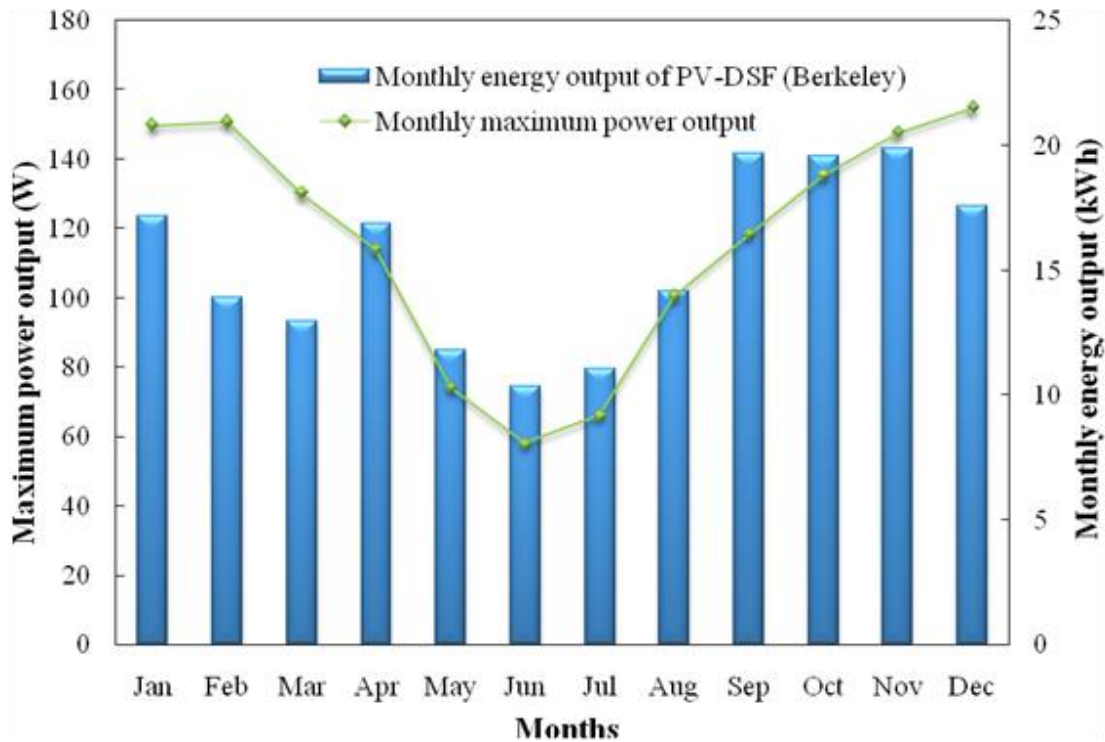
## 287 **5. Overall Energy Performance of PV-DSF in Berkeley**

### 288 **5.1 Power Performance**

289 Based on the sensitivity analysis results given above, the optimized PV-DSF should have  
290 an air gap depth ranging from 400mm to 600mm and operate in the naturally-ventilated  
291 mode. Thus, in this study, a naturally-ventilated PV-DSF with a 400 mm air gap depth  
292 was modeled to investigate the corresponding annual overall energy performance in  
293 Berkeley. The weather data of the typical meteorological year (TMY) were adopted for  
294 the simulation. The annual global solar radiation was about 1692 kWh/m<sup>2</sup> on the  
295 horizontal surface and the incident solar radiation upon the south-facing facade was about  
296 1114 kWh/m<sup>2</sup>.

297 Figure 8 presents the monthly energy output of a south-facing PV-DSF. The monthly  
298 energy output in the winter was about twice that in summer. The maximum monthly  
299 energy output was about 20kWh in November, and the minimum was only 10.3kWh in  
300 June. The total annual energy output of the PV-DSF in Berkeley was about 185kWh.  
301 Figure 8 also presents the maximum transient power output of the PV-DSF for each  
302 month. The results show that the maximum power output, given in December, was 155W,  
303 a figure close to the rated power output of the PV-DSF under standard testing conditions  
304 (170W). The annual energy output per unit area of PV-DSF was 65kWh/m<sup>2</sup> in Berkeley.  
305 The maximum monthly energy output was about 7kWh/m<sup>2</sup>. It is worth noting that the  
306 energy conversion efficiency of the a-Si PV modules used in the PV-DSF was only 6.2%.

307 If high efficiency cadmium telluride (CdTe) PV modules had been adopted, the  
 308 efficiency of which is approximately 10% with a visible light transmittance of 20%, the  
 309 annual energy output of the PV-DSF could be doubled.

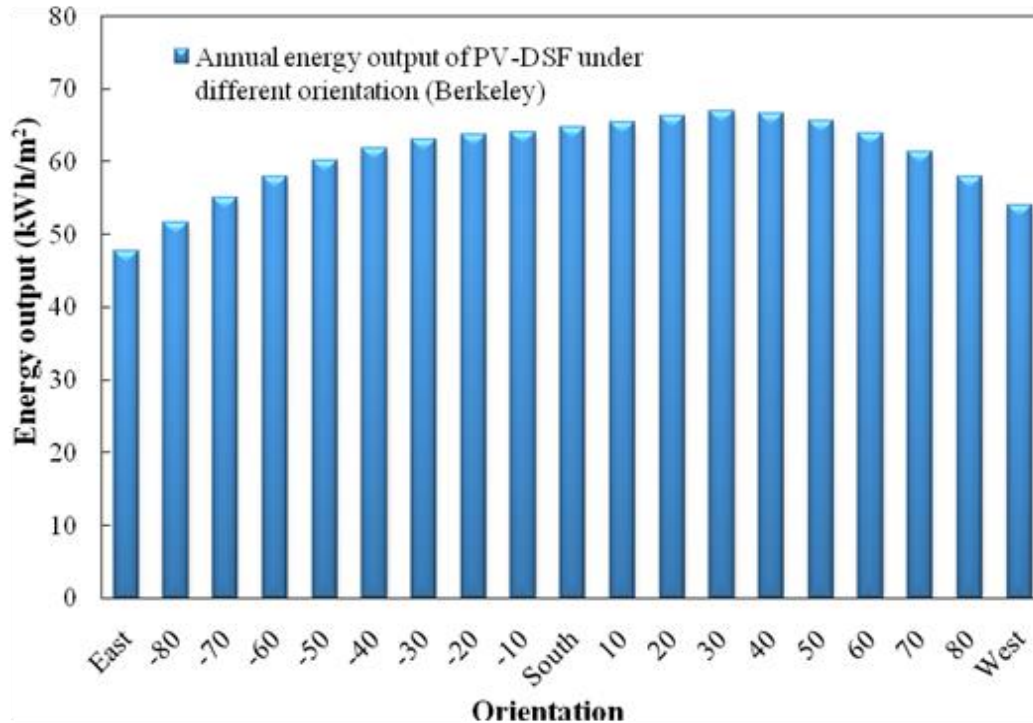


310

311 **Figure 8** Monthly energy output and the maximum power output of PV-DSF

312

313 The best orientation for PV-DSF installation in Berkeley was also determined by  
 314 simulating the annual energy output for different orientations. As shown in Figure 9, if  
 315 evaluation is based only on the power generation performance, the best PV-DSF  
 316 installation orientation for Berkeley is 30 degrees south west, at which the PV-DSF  
 317 generates the most electricity, at about 67kWh/m<sup>2</sup>/yr. In addition, west-facing  
 318 orientations for PV-DSFs in Berkeley have been found to be more suitable for power  
 319 generation, than those which face east.



320

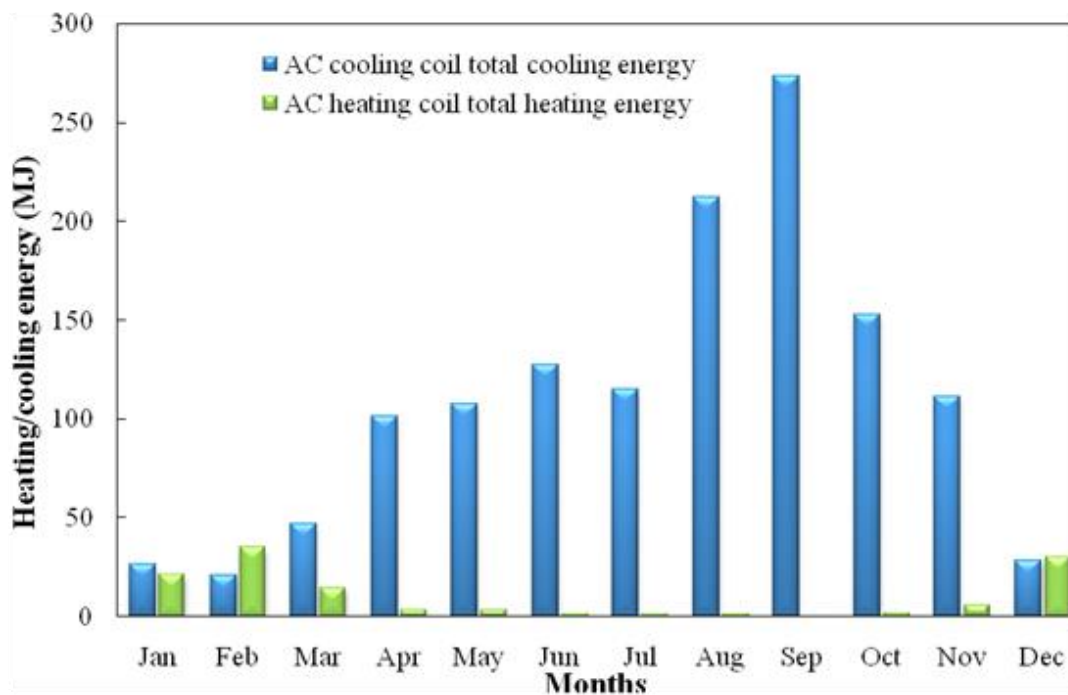
321 **Figure 9** Annual energy output of per unit area of PV-DSFs under different orientations

322 **5.2 Thermal Performance**

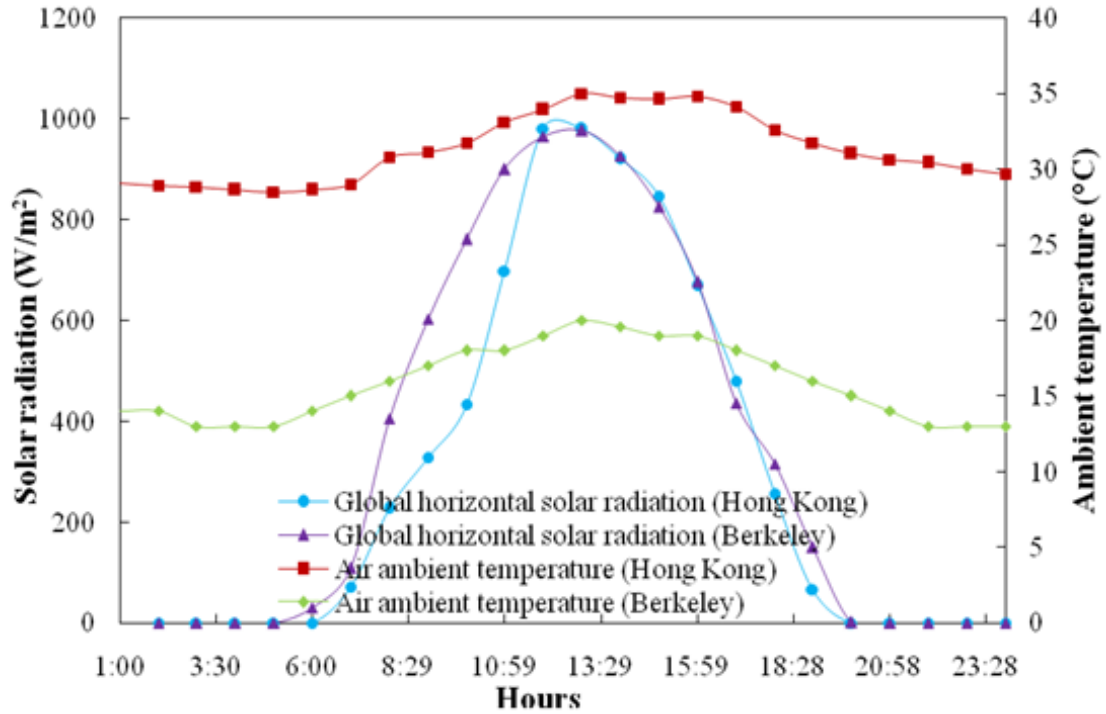
323 Due to the high absorptivity and low transmittance of PV modules, the PV-DSF can  
 324 significantly reduce solar heat gain. It was found that the solar energy passing through the  
 325 PV-DSF was only one seventh of the incident solar energy. Without considering  
 326 convection and thermal radiation, the direct solar heat gain coefficient (DSHGC) of the  
 327 PV-DSF was as low as 0.15 caused by much solar heat gain being blocked by the PV  
 328 modules.

329 Figure 10 presents the monthly demand for cooling energy and heating energy of the  
 330 office room with a PV-DSF installed. Compared with the situation in Hong Kong, the  
 331 monthly demand for cooling energy is much lower in Berkeley. In the latter, the incident  
 332 solar radiation is much higher than that in Hong Kong, but the ambient air temperature is

333 much lower in summer as Berkeley has a cool-summer Mediterranean climate. Weather  
 334 data of a typical summer day in each location was chosen for comparison. Although the  
 335 solar radiation quantities were close, as shown in Figure 11, the ambient air temperature  
 336 in Berkeley was much lower than that in Hong Kong and the minimum temperature  
 337 difference was larger than 13°C. The highest temperature on the typical summer day in  
 338 Berkeley was lower than 25°C, which is the same as the HVAC cooling design  
 339 temperature. Thus, the lower ambient air temperature resulted in a smaller cooling load in  
 340 Berkeley. In addition, the low ambient air temperature aids improvement of the PV  
 341 module's energy efficiency.



342  
 343 **Figure 10** Monthly demand of cooling energy and heating energy of the office room  
 344 installed with PV-DSF



345

346 **Figure 11** Comparison of weather conditions on a typical summer day in Hong Kong and

347

Berkeley

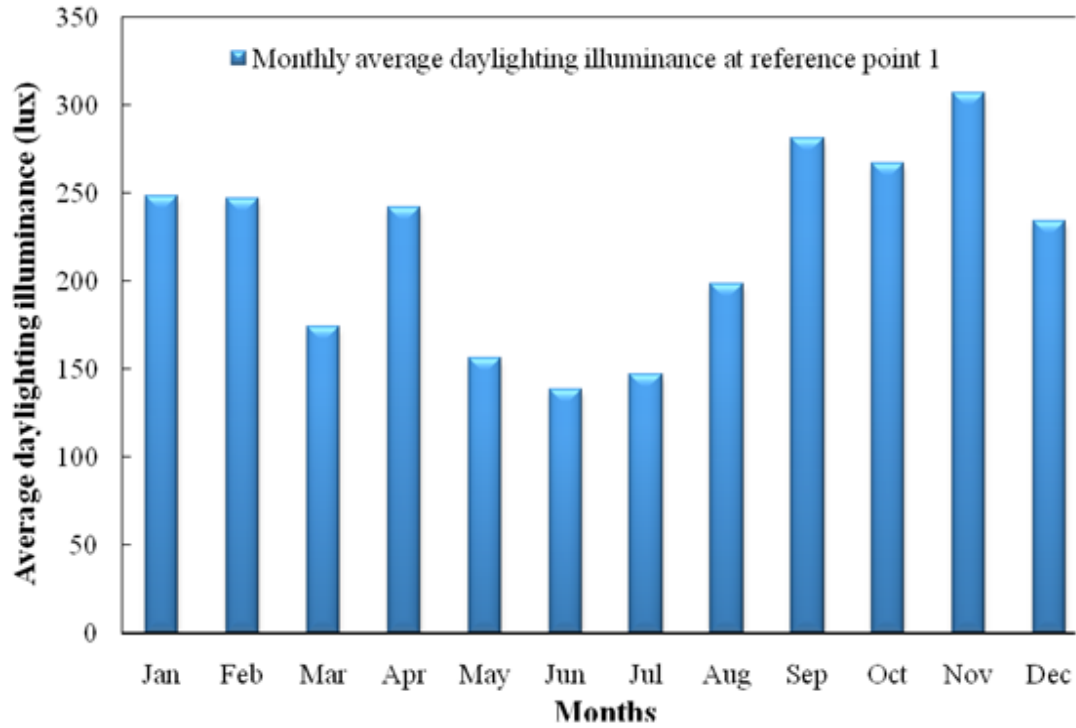
### 348 5.3 Daylighting Performance

349 Figure 12 presents the indoor monthly average daylighting illuminance with the PV-DSF.

350 The maximum monthly average daylighting illuminance was about 300 lux, in November.

351 Such a high daylighting illuminance significantly reduces the artificial lighting energy

352 use.



353

354

**Figure 12** Monthly average daylighting illuminance of PV-DSF in Berkeley

355

Figure 13 presents the monthly average daylighting lighting power multiplier together

356

with the minimum power multiplier for each month. The daylighting lighting power

357

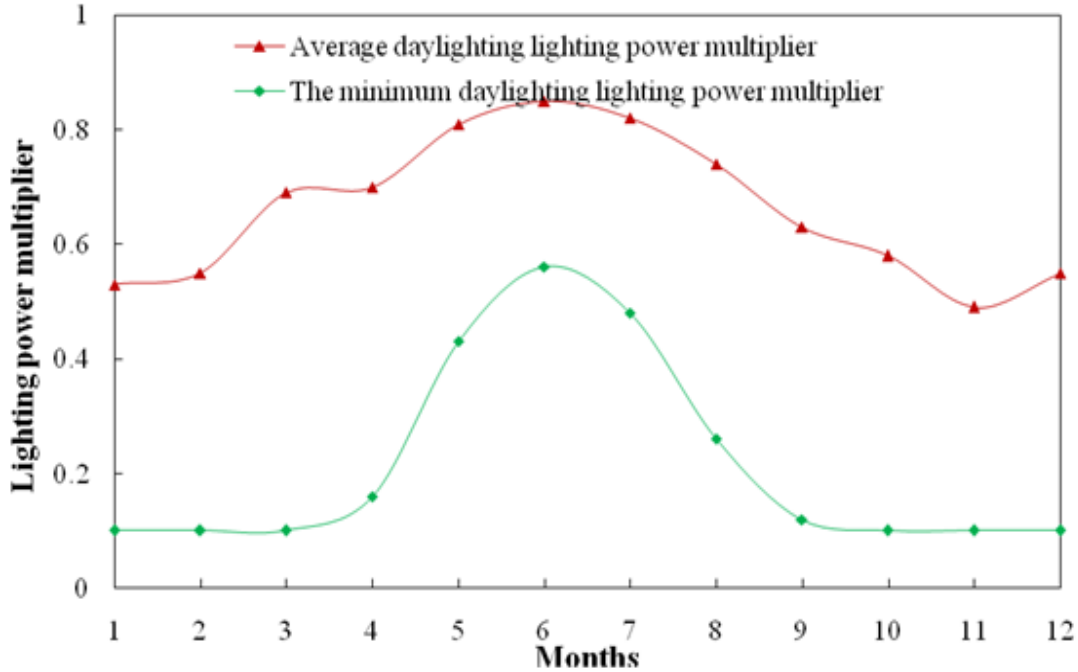
multiplier in winter is obviously lower than in the summer, and about 50% of the lighting

358

electricity can be saved in the winter season. In addition, the minimum daylighting

359

lighting power multiplier, viz. 0.1, appeared in many months.



360

361 **Figure 13** Monthly average daylighting lighting power multiplier and the minimum

362

lighting power multiplier

363

364 The monthly lighting energy use for the office room installed with PV-DSF was

365 calculated and is presented in Figure 14. For comparison, the monthly PV-DSF energy

366 output is also presented. It is seen that the monthly energy output in all months, except

367 for the period May to July, is higher than that of the energy for lighting. Specifically, the

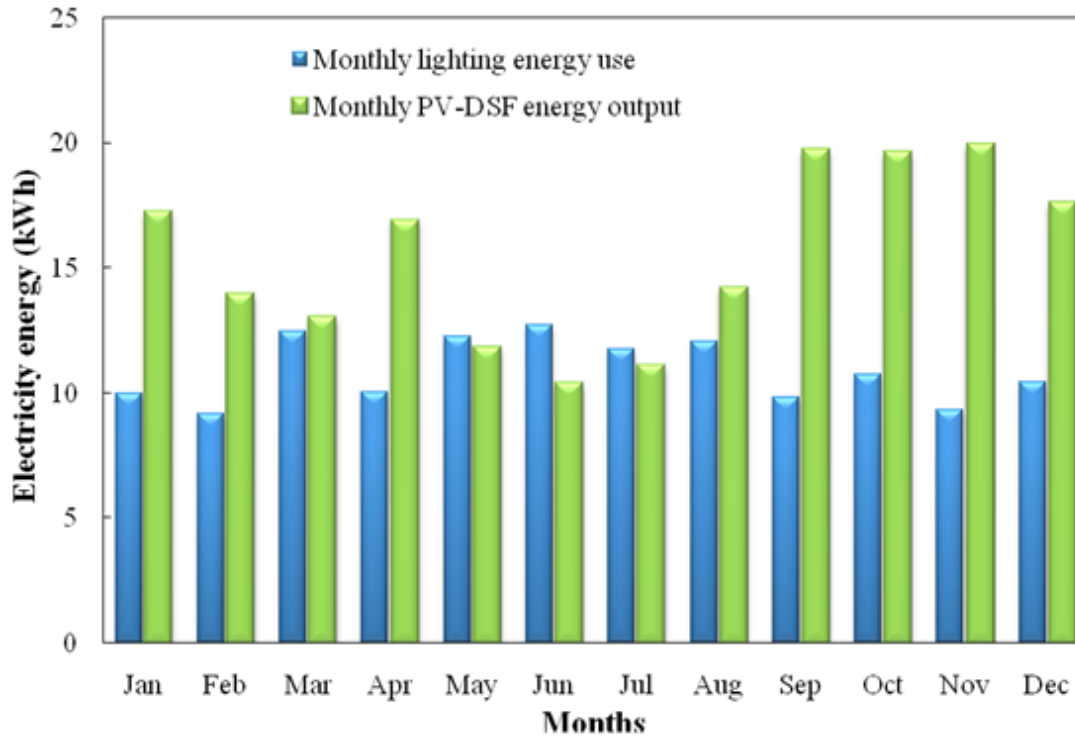
368 energy output in winter is about twice that of the lighting energy used. Thus, in Berkeley

369 the electricity generated by the PV-DSF is sufficient to power the lighting system for

370 most of the year. The total annual energy output of the PV-DSF was about 185kWh,

371 which is higher than the annual lighting energy use by 54kWh.





372

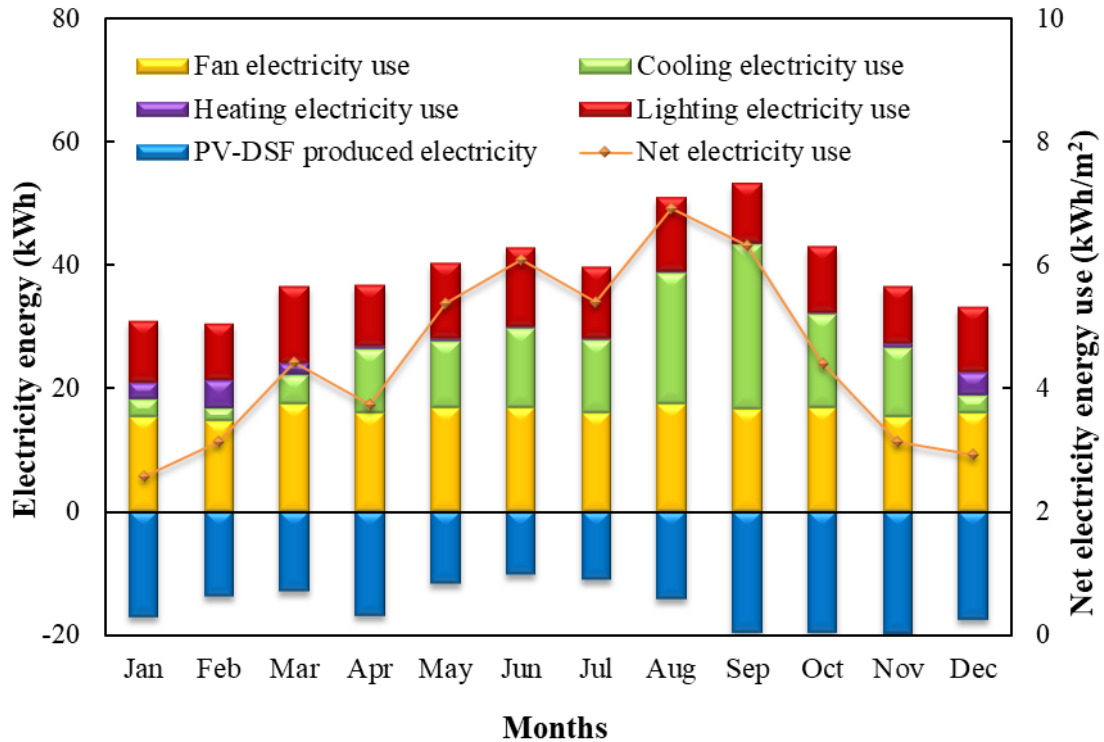
373 **Figure 14** Monthly lighting energy use and energy output of the PV-DSF in Berkeley

374

### 375 **5.4 Overall Energy Performance**

376 The overall energy performance of the PV-DSF, including the thermal, power and  
 377 daylighting performances, are illustrated in Figure 15. It is seen that the largest energy  
 378 consumer over most of the year is the fan. Heating electricity use was very small and can  
 379 be ignored in most months. Two features are also observed in Figure 15. On the one hand,  
 380 the cooling electricity use in Berkeley, is seen to be very low in summer due to the low  
 381 ambient air temperature and on the other hand, the monthly energy output of the PV-DSF  
 382 is high in winter because of the high level of incident solar radiation. The sum of the two  
 383 features given above contributed to the much lower monthly net electricity use for a PV-  
 384 DSF in Berkeley. The minimum monthly net electricity use in January, was only

385 2.6kWh/m<sup>2</sup>. The annual net electricity use in the office was 289kWh, and the net  
 386 electricity use for that room per unit area was only 54.5 kWh/m<sup>2</sup>/yr.



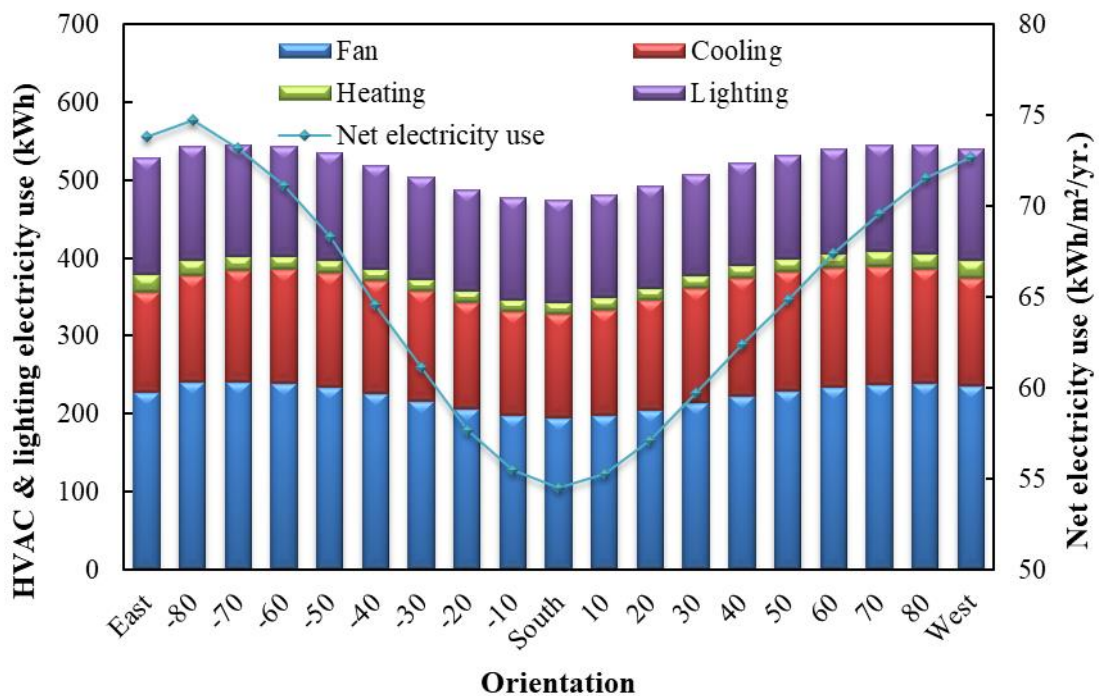
387

388 **Figure 15** Overall energy performance and net electricity use of the PV-DSF

389 As reported above, the summer ambient air temperature in Berkeley, is not high and the  
 390 cooling load is mainly derived from solar heat gain. However, the PV-DSF studied, was  
 391 just sufficiently effective to block solar radiation in the provision of daylighting  
 392 illuminance, therefore greatly reducing the air-conditioning energy use. Apart from its  
 393 passive reduction in energy consumption, PV-DSF can also actively generate enough  
 394 electricity in situ to mitigate the load on the utility grid and further reduce the total net  
 395 electricity use of buildings.

396 The optimum orientation in terms of power generation for a PV-DSF installation in  
 397 Berkeley was found to be 30 degrees south west. It is necessary to find the best

398 orientation to enable the overall energy consumption for a PV-DSF installation to be  
 399 achieved. The annual HVAC & lighting electricity uses of PV-DSFs for different  
 400 orientations in Berkeley is presented in Figure 16. It is found that an office room facing  
 401 due south consumes the least electricity. The room's annual net electricity use was  
 402 calculated by taking the total annual energy output into account. As shown in Figure 16,  
 403 due south is the optimum orientation for a PV-DSF installation because this orientation  
 404 requires the lowest net electricity use. Compared with the worst orientation, viz. 10  
 405 degrees east by south, a due south facing PV-DSF could save 107kWh electricity per year  
 406 in Berkeley, about 37kWh/yr. for per unit area.



407

408 **Figure 16** The total and net electricity uses of PV-DSFs under different orientations in  
 409 Berkeley

410 **6. Energy Saving Potential of PV-DSF**

411 Although the annual overall PV-DSF energy performance has been demonstrated above,  
 412 the energy saving potential of a PV-DSF compared with other types of windows and  
 413 facade systems is still unclear. Thus, a study was conducted to compare the overall  
 414 energy performances of a PV-DSF and six commonly used glazing systems (windows  
 415 and facade systems). The glazing systems and the corresponding scenarios chosen for this  
 416 study are listed in Table 4. The structures of various glazing systems as well as the glass  
 417 IDs, as in the international glazing database (IGDB), are also given in Table 4.

418 Figure 17 presents the annual electricity use of office rooms fitted with different types of  
 419 windows and facades in Berkeley. It is seen that Scenarios E and G (PV-DSF) consume  
 420 much less cooling electricity, and their total electricity uses were much lower than the  
 421 others. Even without taking the PV power generation into account, the PV-DSF (Scenario  
 422 G) was almost the most energy efficient choice in Berkeley. Its annual total electricity  
 423 use was 473kWh, just a little higher than that of Scenario E. However, if the annual PV  
 424 power generation of about 185kWh is also counted, the annual net electricity use of the  
 425 PV-DSF (Scenario G) was as low as 288.7kWh, much lower than the other types of  
 426 windows and facades. As mentioned above, if high efficiency semi-transparent CdTe PV  
 427 modules were to be adopted in this kind of PV-DSF, the annual energy output could be  
 428 doubled. With the improved efficiency of semi-transparent PV modules, the advantages  
 429 of PV-DSF will become larger in the future, making this a very promising energy-  
 430 efficient facade for Berkeley.

431 **Table 4** Information of the chosen glazing systems

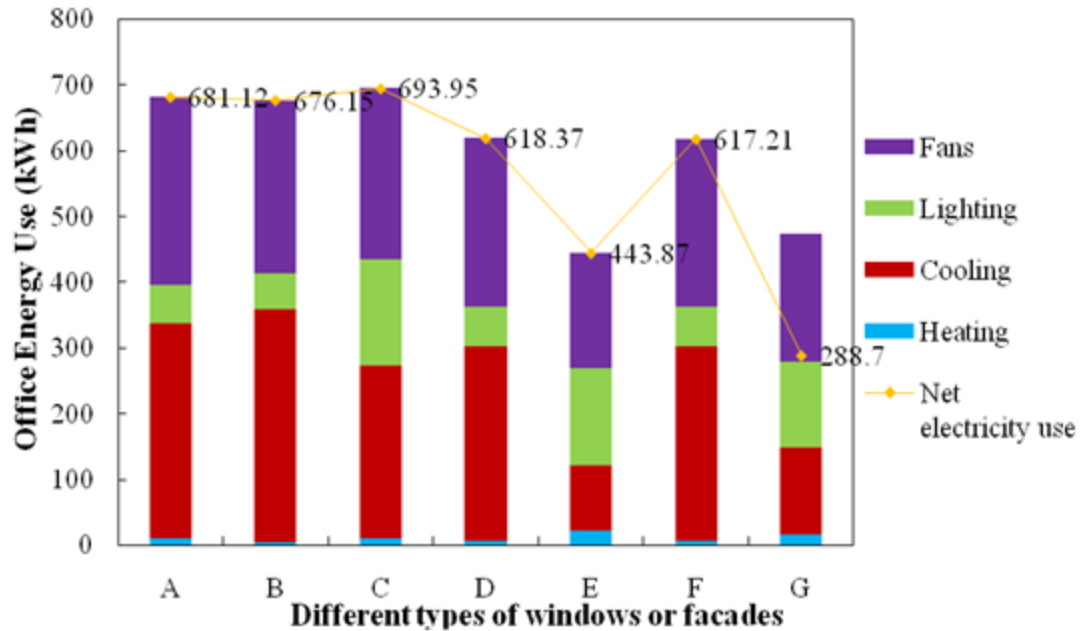
Scenarios	Glazing name	Structure	ID in IGDB	Note
-----------	--------------	-----------	---------------	------

<b>A</b>	Double bronze	Bronze(5.61mm)+Air gap(12.7mm)+Clear(5.66mm)	898/9804	
<b>B</b>	Double low solar low-e clear	SB60 clear(5.66mm)+Air gap(12.7mm)+Clear(5.66mm)	5284/9804	
<b>C</b>	Double clear with shading always on	Clear(5.72mm)+Air gap(12.7mm)+Clear(5.72mm)	103/103	"always on" means the VB always cover the window
<b>D</b>	DSF clear glass with shading always off	Clear(5.72mm)+Air ventilation duct(400mm)+Clear(3mm)	103/412	"always off" means the VB always cover none of the window
<b>E</b>	DSF clear glass with shading always on	Clear(5.72mm)+Air ventilation duct(400mm)+Clear(3mm)	103/412	
<b>F</b>	DSF clear glass with shading on if high glare	Clear(5.72mm)+Air ventilation duct(400mm)+Clear(3mm)	103/412	"on if high glare" means the VB cover the window when the glare is high
<b>G</b>	<b>PV-DSF</b> PV laminate	a-Si PV laminate(8mm)+Air ventilation duct(400mm)+Clear(3mm)	60900/412	

---

432

433



434

435 **Figure 17** Net electricity uses of office rooms fitted with different types of windows or  
 436 facades in Berkeley

437

438 **7. Conclusions**

439 A comprehensive simulation model based on EnergyPlus has been developed and  
 440 introduced in this paper. The model can be used to simulate the annual overall energy  
 441 performance of a ventilated PV-DSF in a cool-summer Mediterranean climate zone.

442 Using the simulation model, sensitivity analyses of air gap depths and modes of  
 443 ventilation were conducted to investigate their impact on overall energy performance. It  
 444 was found that the least efficient air gap depth for PV-DSF installation was 200 mm. At  
 445 this gap depth the most electricity was consumed by the room. After a comprehensive  
 446 analysis of all aspects relating to energy generation, cost, space utilization and  
 447 maintenances, it was concluded that thicknesses between 400 and 600mm could be

448 recommended as the optimal air gap range for a PV-DSF installation in Berkeley. About  
449 15% of the annual net electricity use could be saved if an air gap depth of 600mm rather  
450 than 200mm was chosen. It was found that ventilation modes also significantly affect the  
451 overall energy performance of a PV-DSF. When compared with a non-ventilated PV-  
452 DSF, the naturally-ventilated PV-DSF saves about 35% of electricity use per year in  
453 Berkeley, a situation which is a powerful indication that the consideration of ventilation  
454 design is a necessary undertaking in the production of the most effective PV-DSF  
455 solution in terms of energy saving.

456 The PV-DSF was able to generate about 65kWh per unit area, electricity yearly in  
457 Berkeley. If high efficiency cadmium telluride (CdTe) semi-transparent PV modules  
458 were to be adopted, the annual energy output of the PV-DSF could be doubled. The PV-  
459 DSF studied also produced good thermal and daylighting performances. Except for  
460 providing considerable interior daylight, the PV-DSF was able to effectively block solar  
461 radiation from the interior. The direct solar heat gain coefficient (DSHGC) of the PV-  
462 DSF was as low as 0.15, without considering convection and thermal radiation. The  
463 maximum monthly average daylighting illuminance was about 300 lux, enabling about  
464 50% of lighting electricity to be saved in winter. The electricity generated by the PV-DSF  
465 was sufficient to power the lighting system for most of the year.

466 The overall energy performance of the PV-DSF in Berkeley was evaluated and two  
467 specific features were observed. On the one hand, cooling electricity use was low in  
468 summer due to the low ambient air temperature; and on the other hand, the monthly  
469 energy output was large over the whole year because of the abundance of solar radiation.  
470 The above two factors, together, contributed to the low net electricity use figure for a PV-

471 DSF in Berkeley. The annual net electricity use per unit area in the office room was only  
472 54.5 kWh/m<sup>2</sup>, and the minimum monthly net electricity use was only 2.6kWh/m<sup>2</sup>.

473 A comparative study was also conducted to evaluate the energy saving potential of  
474 various window and facade designs in Berkeley. The results showed that the PV-DSF  
475 used about 50% less net electricity than other commonly used glazing systems. With the  
476 improved efficiency of semi-transparent PV modules, it appears clear that the energy  
477 saving potential of PV-DSFs will become increasingly attractive in future. Thus, it  
478 appears clear that PV-DSF provides promising energy-efficient facade for Berkeley and  
479 therefore possibly, for other areas with the characteristics of abundant solar energy  
480 resources and a cool-summer Mediterranean climate.

481

#### 482 **Acknowledgements**

483 The authors appreciate the financial supports provided by the Public Policy Research  
484 (PPR) Funding Scheme 2013/14 (PPR Project: 2013.A6.010.13A) of the Hong Kong  
485 Special Administrative Region (HKSAR), the Hong Kong Construction Industry Council  
486 Research Fund (CIC Project: K-ZJK1), the Fundamental Research Funds for the Central  
487 Universities (Hunan University), as well as the Hong Kong Housing Authority Research  
488 Fund (Project no. K-ZJHE).

489

#### 490 **References**

- 491 [1] 2011 Buildings Energy Data Book. Buildings Technologies Program Energy  
492 Efficiency and Renewable Energy, U.S. Department of Energy. March 2012. <  
493 [http://buildingsdatabook.eren.doe.gov/docs/DataBooks/2011\\_BEDB.pdf](http://buildingsdatabook.eren.doe.gov/docs/DataBooks/2011_BEDB.pdf) >  
494 [2] Yoon JH, Shim SR, An YS, Lee KH. An experimental study on the annual surface  
495 temperature characteristics of amorphous silicon BIPV window. *Energy and*  
496 *Buildings* 2013; 62: 166–175.



- 497 [3] Han J, Lu L, Peng JQ, Yang HX. Performance of ventilated double-sided PV façade  
498 compared with conventional clear glass façade. *Energy and Buildings* 2013; 56: 204-  
499 209.
- 500 [4] Chen FZ, Wittkopf SK, Ng PK, Du H. Solar heat gain coefficient measurement of  
501 semi-transparent photovoltaic modules with indoor calorimetric hot box and solar  
502 simulator. *Energy and Buildings* 2012; 53: 74–84.
- 503 [5] Fung YY, Yang HX. Study on thermal performance of semi-transparent building-  
504 integrated photovoltaic glazings. *Energy and Buildings* 2008; 40: 341-350.
- 505 [6] Park KE, Kang GH, Kim HI, Yu GJ, Kim JT. Analysis of thermal and electrical  
506 performance of semi-transparent photovoltaic (PV) module. *Energy* 2010; 35: 2681-  
507 2687.
- 508 [7] Xu S, Liao W, Huang J, Kang J. Optimal PV cell coverage ratio for semi-transparent  
509 photovoltaic on office building facades in central China. *Energy and Buildings* 2014;  
510 77: 130–138.
- 511 [8] Han J, Lu L, Yang HX. Thermal behavior of a novel type see-through glazing system  
512 with integrated PV cells. *Building and Environment* 2009; 44: 2129–2136.
- 513 [9] Yoon JH, Song JH, Lee SJ. Practical application of building integrated photovoltaic  
514 (BIPV) system using transparent amorphous silicon thin-film PV module. *Solar*  
515 *Energy* 2011; 85: 723-733.
- 516 [10] Han J, Lu L, Yang HX. Numerical evaluation of the mixed convective heat transfer  
517 in a double-pane window integrated with see-through a-Si PV cells with low-e  
518 coatings. *Applied Energy* 2010; 87: 3431-3437.
- 519 [11] Bizzarri, G., Gillott, M., & Belpoliti, V. (2011). The potential of semitransparent  
520 photovoltaic devices for architectural integration. *Sustainable Cities and Society*, 1(3),  
521 178–185. doi:10.1016/j.scs.2011.07.003
- 522 [12] López, C. S. P., & Sangiorgi, M. (2014). Comparison Assessment of BIPV Façade  
523 Semi-transparent Modules: Further Insights on Human Comfort Conditions. *Energy*  
524 *Procedia*, 48(0), 1419–1428. doi:10.1016/j.egypro.2014.02.160
- 525 [13] Peng J, Lu L, Yang H. Review on life cycle assessment of energy payback and  
526 greenhouse gas emission of solar photovoltaic systems. *Renewable and Sustainable*  
527 *Energy Reviews* 2013; 19: 255-274.
- 528 [14] Lu L, Law KM. Overall energy performance of semi-transparent single-glazed  
529 photovoltaic (PV) window for a typical office in Hong Kong. *Renewable Energy*  
530 2013; 49: 250-254.
- 531 [15] Miyazaki T, Akisawa A, Kashiwagi T. Energy savings of office buildings by the use  
532 of semi-transparent solar cells for windows. *Renewable Energy* 2005; 30: 281–304.
- 533 [16] Chow TT, Li CY, Lin Z. Innovative solar windows for cooling-demand climate.  
534 *Solar Energy Materials and Solar Cells* 2010; 94:212-220.
- 535 [17] Wong PW, Shimoda Y, Nonaka M, Inoue M, Mizuno M. Semi-transparent PV:  
536 Thermal performance, power generation, daylight modelling and energy saving  
537 potential in a residential application. *Renewable Energy* 2008; 33: 1024-1036.
- 538 [18] Peng J, Lu L, Yang H, Han J. Investigation on the annual thermal performance of a  
539 photovoltaic wall mounted on a multi-layer façade. *Applied Energy* 2013;112:646-  
540 656.

- 541 [19] Cuce E, Young CH, Riffat SB. Thermal performance investigation of heat insulation  
542 solar glass: A comparative experimental study. *Energy and Buildings* 2015; 86:595–  
543 600.
- 544 [20] Ng, P. K., & Mithraratne, N. (2014). Lifetime performance of semi-transparent  
545 building-integrated photovoltaic (BIPV) glazing systems in the tropics. *Renewable  
546 and Sustainable Energy Reviews*, 31, 736–745. doi:10.1016/j.rser.2013.12.044
- 547 [21] Lynn, N., Mohanty, L., & Wittkopf, S. (2012). Color rendering properties of semi-  
548 transparent thin-film PV modules. *Building and Environment*, 54, 148–158.  
549 doi:10.1016/j.buildenv.2012.02.010
- 550 [22] Li, D. H. W., Lam, T. N. T., & Cheung, K. L. (2009). Energy and cost studies of  
551 semi-transparent photovoltaic skylight. *Energy Conversion and Management*, 50(8),  
552 1981–1990. doi:10.1016/j.enconman.2009.04.011
- 553 [23] Chow, T. T., Fong, K. F., He, W., Lin, Z., & Chan, a. L. S. (2007). Performance  
554 evaluation of a PV ventilated window applying to office building of Hong Kong.  
555 *Energy and Buildings*, 39(6), 643–650. doi:10.1016/j.enbuild.2006.09.014
- 556 [24] Ng, P. K., Mithraratne, N., & Kua, H. W. (2013). Energy analysis of semi-  
557 transparent BIPV in Singapore buildings. *Energy and Buildings*, 66, 274–281.  
558 doi:10.1016/j.enbuild.2013.07.029
- 559 [25] Li, D. H. W., Lam, T. N. T., Chan, W. W. H., & Mak, A. H. L. (2009). Energy and  
560 cost analysis of semi-transparent photovoltaic in office buildings. *Applied Energy*,  
561 86(5), 722–729. doi:10.1016/j.apenergy.2008.08.009
- 562 [26] Motuziene V, Bielskus J. Assessment of overall performance of building integrated  
563 photovoltaics. The 9th International Conference on Environmental Engineering. 22–  
564 23 May 2014, Vilnius, Lithuania.
- 565 [27] Olivieri, L., Caamaño-Martín, E., Moralejo-Vázquez, F. J., Martín-Chivelet, N.,  
566 Olivieri, F., & Neila-Gonzalez, F. J. (2014). Energy saving potential of semi-  
567 transparent photovoltaic elements for building integration. *Energy*, 76, 572–583.  
568 doi:10.1016/j.energy.2014.08.054
- 569 [28] Leite Didoné, E., & Wagner, A. (2013). Semi-transparent PV windows: A study for  
570 office buildings in Brazil. *Energy and Buildings*, 67, 136–142.  
571 doi:10.1016/j.enbuild.2013.08.002
- 572 [29] Chae, Y. T., Kim, J., Park, H., & Shin, B. (2014). Building energy performance  
573 evaluation of building integrated photovoltaic (BIPV) window with semi-transparent  
574 solar cells. *Applied Energy*, 129, 217–227. doi:10.1016/j.apenergy.2014.04.106
- 575 [30] Kapsis K, Athienitis AK. A study of the potential benefits of semi-transparent  
576 photovoltaics in commercial buildings. *Solar Energy* 2015; 115: 120-132.
- 577 [31] Olivieria L, Caamano-Martina E, Olivierib F, Neila J. Integral energy performance  
578 characterization of semi-transparent photovoltaic elements for building integration  
579 under real operation conditions. *Energy and Buildings* 2014; 68: 280–291.
- 580 [32] Pal SK, Alanne K, Jokisalo J, Siren K. Energy performance and economic viability  
581 of advanced window technologies for a new Finnish townhouse concept. *Applied  
582 Energy* 2016; 162: 11–20.
- 583 [33] Chow, T.-T., Qiu, Z., & Li, C. (2009). Potential application of “see-through” solar  
584 cells in ventilated glazing in Hong Kong. *Solar Energy Materials and Solar Cells*,  
585 93(2), 230–238. doi:10.1016/j.solmat.2008.10.002

- 586 [34] Brandl D, Mach T, Grobbauer M, Hochenauer C. Analysis of ventilation effects and  
587 the thermal behaviour of multifunctional facade elements with 3D CFD models.  
588 Energy and Buildings 2014; 85: 305–320.
- 589 [35] He, W., Zhang, Y. X., Sun, W., Hou, J. X., Jiang, Q. Y., & Ji, J. (2011).  
590 Experimental and numerical investigation on the performance of amorphous silicon  
591 photovoltaics window in East China. Building and Environment, 46(2), 363–369.  
592 doi:10.1016/j.buildenv.2010.07.030
- 593 [36] Elarga H, Zarrella A, De Carli M. Dynamic energy evaluation and glazing layers  
594 optimization of facade building with innovative integration of PV modules, Energy  
595 and Buildings (2015), <http://dx.doi.org/10.1016/j.enbuild.2015.11.060>
- 596 [37] Peng JQ, Lu L, Yang HX. An experimental study of the thermal performance of a  
597 novel photovoltaic double-skin facade in Hong Kong. Solar Energy 2013; 97: 293-  
598 304.
- 599 [38] Peng JQ, Lu L, Yang HX, Ma T. Comparative study of the thermal and power  
600 performances of a semi-transparent photovoltaic façade under different ventilation  
601 modes. Applied Energy 2015; 138: 572-583.
- 602 [39] Mitchell R., Kohler C., Klems J., Rubin M, Arasteh D. WINDOW 6.1 / THERM 6.1  
603 Research Version User Manual. Lawrence Berkeley National Laboratory, US. 2006.
- 604 [40] King, D., Boyson, W., Kratochvill, J., 2004. Photovoltaic Array Performance Model.  
605 Sandia Report 2004-3535, Sandia National Laboratories, Albuquerque, NM.
- 606 [41] Peng J, Lu L, Yang H, Ma T. Validation of the Sandia model with indoor and  
607 outdoor measurement for semi-transparent amorphous silicon PV module. Renewable  
608 Energy 2015; 80: 316-323.
- 609 [42] King, D., Kratochvil, J., Boyson, W., 1997a. Measuring Solar Spectral and Angle-  
610 of-Incidence Effects on PV Modules and Solar Irradiance Sensors. 26th IEEE PV  
611 Specialists Conference 1997: 1113-1116.
- 612 [43] King, D., Kratochvil, J., Boyson, W., 1997b. Temperature Coefficients for PV  
613 Modules and Arrays: Measurement Methods, Difficulties, and Results. 26th IEEE PV  
614 Specialists Conference 1997: 1183-1186.
- 615